Good thermoelectric performance and stability in copper sulfide synthesized by hydrothermal method and densified by HP technique

Feng Liu[1], He Yu[1], Jian Fu[1], and Xiaowei Zhang[1,*] (iD)

[1] State Key Laboratory of Environment-Friendly Energy Materials, Southwest University of Science and Technology, Mianyang 621010, China

ABSTRACT

We investigate the thermoelectric performance and the stability of polycrystalline *p*-type $Cu_{2-x}S$ fabricated by hydrothermal method and hot-pressing technique. The relative pure copper sulfides are obtained via the sintering process and their crystal structures are dependence on the atomic ratio of Cu/S. The thermoelectric performance tests show a good figure of merit of $ZT = 0.78$ at 550 °C. In addition, we repeated measured the thermoelectric parameters to confirm the stability of the samples. The electrical conductivity and the Seebeck coefficient have dramatically change between the different tests, which originate from the variation of carrier concentration and mobility. Nonetheless, the figure of merit ZT maintains unchanged, indicating that the samples synthesized in this work possess quite stable thermoelectric performance.

1 Introduction

Thermoelectric (TE) materials can realize the direct interconvert between the thermal and electric energy and have been investigated extremely during the past two decades [1–7]. The converting coefficient for the TE application of power generation or cooling is determined by the dimensionless figure of merit $ZT = S^2\sigma T/\kappa$, where S, σ, T and κ are the Seebeck coefficient, electrical conductivity, thermodynamic temperature and thermal conductivity, respectively. High ZT value means high energy conversion efficiency, requiring high power factor ($PF = S^2\sigma$) and low thermal conductivity κ synchronously.

Therefore, most of previous studies in TE materials are focus on how to improve the ZT value through doping, composite technique, low-dimensional etc. or searching new intrinsic high ZT materials [8–17].

Currently, traditional TE materials with high ZT value include Si–Ge alloy, telluride systems, etc. Si-Ge alloy are one of the most important TE materials working usually in the field of high temperature, with high PFs and antioxidant capacity. Recently, Si-Ge nanowires as thermoelectric generator also receive many attention due to the higher TE performance related to their bulk crystal counterparts over the low temperature range from 273 to 450 K. However, the intrinsic high thermal conductivity in Si-Ge alloy

Address correspondence to E-mail: xiaoweizhang@swust.edu.cn; hedge80@sina.com.cn

 Springer

poses a challenge to higher *ZT* values [18–22]. Telluride systems are now widely used commercially, but most of them contain valuable and toxic elements [9, 12, 23, 24]. In the consideration of searching low cost, eco-friendly and intrinsic high *ZT* values TE materials, copper sulfides have been widely investigated and the TE performance also improve constantly in the past decade [4, 25–29]. For example, a very high *ZT* value up to 1.9 in $Cu_{1.97}S$ system at 700 °C was obtained by Zhao [30] et al. who synthesized the specimen with the melt-solidification technique. He [31] et al. also explored TE characteristics of $Cu_{2-x}S$ and obtained quite high *ZT* values of 1.4–1.7 around 1000 K with vacuum melting. Cu-S based composites also show a good thermoelectric performance. The containing materials often include In_2S_3 [32, 33], AgCl [34], $CoSb_3$ [35], Se [36, 37], etc. and the related *ZT* values are also found between 1 and 2.

However, as a kind of liquid-like materials, the working stability of copper sulfides must be considered because Cu^+ exhibits a migrating behavior under a bias voltage. In the Cu-S based structures, carrier concentration (*n*) contains two parts: n_{Cu+} and n_{hole}. Cu^+ migration can reduce *n* and leave simultaneously a lot of point defects in the matrix, which will affect the *σ* and then the *ZT* of copper sulfides [26, 38–42]. Therefore, in this work, we synthesize $Cu_{2-x}S$ samples via the hydrothermal method and hot-pressing (HP) technique and investigate their TE performance and the working stability. The previous literatures present a lot of synthesis methods, such as vacuum melting [43], mechanical alloying [44, 45], hydrothermal synthesis [45, 46] and thermal decomposition [47]. Among them, the vacuum melting method can yield high *ZT* values in copper sulfides, but need high melting temperatures and long annealing time. On the contrary, chemical synthesis techniques, like the hydrothermal method, can synthesize directly crystalline $Cu_{2-x}S$ powders with small grain size at relative low temperature. For energy saving, chemical synthesis techniques is the better choice.

2 Experiments

In this work, $Cu_{2-x}S$ powders were prepared by hydrothermal method and the bulk samples were sintered by HP technique. High purity powders of CuCl (99.99%, Aladdin) and of $CS(NH_2)_2$ (98.0%,

Cologne) were used as sources of copper and sulfur. Firstly, dissolving 0.9 g of CuCl powders and 1.2 g of $CS(NH_2)_2$ powders into 40ml mixture of anhydrous ethanol and distilled water (in volume ratio of 9:1). The solution was then transferred into a Teflon-lined stainless steel autoclave and sealed. The autoclave was heated to 180 °C for 16 h and then cooled down to room temperature naturally. The product was collected carefully by centrifuging and dried at 60 °C for 10 h and then washed with distilled water and anhydrous ethanol. This process was repeated several times and then the copper sulfide compound powders were obtained. Finally, the prepared powders were sintered in vacuum by HP technique. In this work, we set up three group of sintering parameters and the corresponding bulk samples are marked as S1, S2 and S3. The specific parameters can be referred to Fig. 1. The disk shape of $Cu_{2-x}S$ bulk samples then was cut into blocks for the performance testing. The phase structures of the powders and bulk samples were identified by an X-ray diffractometer (XRD, X Pert pro X, Netherlands). The morphology of the powders and the cross-sections of the bulk samples were observed by using a field emission scanning electron microscope (FESEM, SUPRA 55, Carl Zeiss, Oberkochen, Germany). The electrical performance was measured by a CTA-3 system (Cryoall, China) from 30 to 550 °C in helium atmosphere. For getting the thermal conductivity, the density *ρ*, thermal diffusion coefficient *D* and specific heat capacity C_p of the bulk samples were tested by the Archimedes method, laser flash method (DLF-
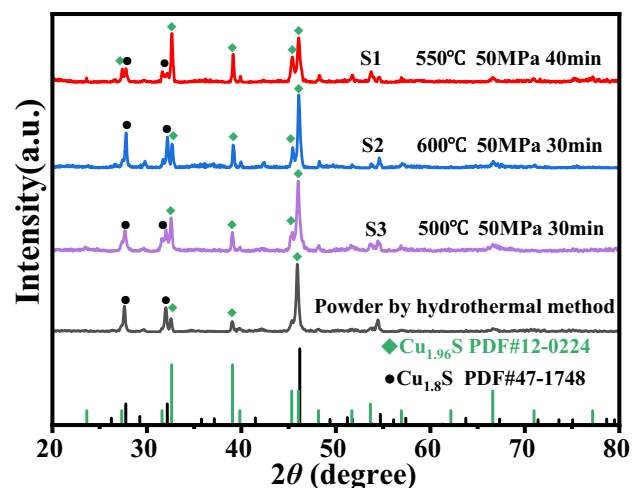

Fig. 1 XRD patterns of the hydrothermal $Cu_{2-x}S$ powders and the bulk samples

1600, American) and differential scanning calorimetry (DSC, Q2000 V24.11 Build 124, American) respectively. The desired thermal conductivity was then calculated with formula $\kappa = \rho D C_p$.

3 Results and discussions

The XRD pattern of the powders prepared by hydrothermal method is displayed in Fig. 1. Compared to the ICDD files No. 12-0224 and No. 47-1748, the powder seems to be a mixture containing digenite phase and djurleite phase, which may be due to the sensitive dependence on Cu/S atomic ratio in the crystal structures of copper sulfides. For the sintered bulk samples, however, the diffraction peaks belonging to djurleite phase become more and more intensive with the sintering temperature raising and the time prolonging, indicating the crystal structure transforms from digenite phase to djurleite phase due to the sulfur volatilization during the sintering process. In this work, the sample S1, which sintered at 550 °C and under 50 MPa for 40 min, has the purest djurleite phase as clearly shown in Fig. 1. According to some previous reports [27, 31, 38, 42, 48, 49], $Cu_{2-x}S$ in djurleite phase has better thermoelectric performance, which also be confirmed in the present work below.

The typical micrographs of powders and the cross-sections of bulk samples were displayed in Fig. 2. The prepared powders possess beautiful flower sphere shape with diameter range from a few hundred nanometers to several micrometers. These flower spheres are assembled by lots of nanoflakes as clearly observed in Fig. 2a and the corresponding zoomed in Figs. [50, 51]. The morphologies of $Cu_{2-x}S$ powders are heavily dependent on the hydrothermal temperature and drying temperature [51]. Figure 2b–d shows the fracture surfaces of the sintered samples. Clearly, the samples S1 and S3 have homogeneous grain size with around 200 *nm* in diameter, while the sample S2 exhibits abnormal grain growth with most grain sizes over 1 μm. This is due to the high sintering temperature in sample S2. The large grain size may not be conducive to enhance the phonon scattering and hence increase the TE performance [1, 49].

The temperature-dependent electrical properties of the polycrystalline bulk $Cu_{2-x}S$ samples is shown in Fig. 3a–c. Very clearly, these samples show a metallic behavior at relative low temperature range, while show a semiconducting behavior at the high temperature range. The turning temperature is around 150 °C. The peak σ value of samples S1 and S2 reaches up to $16 \times 10^4 \, Sm^{-1}$, which is larger than that of most previous studies [3, 29–31]. Sample S3, by contrast, has a lower peak σ value of $14 \times 10^4 \, Sm^{-1}$. This result may be due to the better crystallization in sample S1 and S2 as clearly seen in Fig. 2. Generally, the larger σ results in the smaller Seebeck coefficient S. In this work, sample S3 really exhibits larger S than the other two samples. The peak S value reaches up to 190 μV/K as shown in Fig. 3b. In addition, all Seebeck coefficient S show a positive value, indicating the $Cu_{2-x}S$ sample is a *p*-type semiconductor. However, for these three samples, the determining power factors (*PFs*) have not showed an obvious difference over the testing temperature range, indicating that the sintering conditions in this work have slight influence on *PF*. We compared our *PFs* with those of the previous studies on the copper sulfide structures, most of which are the doping or composite systems for improving the TE performance. The *PF* value of 9.98 μW/(cm·K^2) in this work is quite good, as can be seen in Fig. 3d. Some doping and composite copper sulfide analogs exhibit high power factors [30, 33, 37, 52–54]. For instance, Ge [32] et al. composited 3% In_2S_3 into main matrix of $Cu_{1.8}S$ and the *PF* reaches up to 11 μW cm^{-1} K^{-2}. In this work, however, we synthesized relative pure $Cu_{2-x}S$ bulk samples by the hydrothermal approach, achieving a quite high *PF*. Note that we here only show the *PF* of sample S1 because all samples exhibit almost the same *PF* value.

For evaluating the TE performance of our samples, excellent electrical properties are not enough. Low thermal conductance κ is also necessary. The tested results of κ is shown in Fig. 4a. The sample S2 shows very large κ, which is almost three times larger than sample S1. This must be due to the large grain size in sample S2 (see Fig. 2c). In copper sulfide structures, the phonon scattering with moderate wavelength dominates the process of lattice thermal transport. The samples S1 and S3, therefore, have a smaller κ due to smaller grain size. However, because of the better crystallization, the sample S1 has the optimal κ and hence certainly have optimal figure of merit *ZT* by considering almost the same *PFs* among three samples. The calculated *ZT* value for three samples is showed in Fig. 4b. Expectedly, sample S1 has the

Fig. 2 FESEM images of the hydrothermal $Cu_{2-x}S$ powders (**a**) and the bulk samples of S1(**b**), S2(**c**) and S3(**d**)
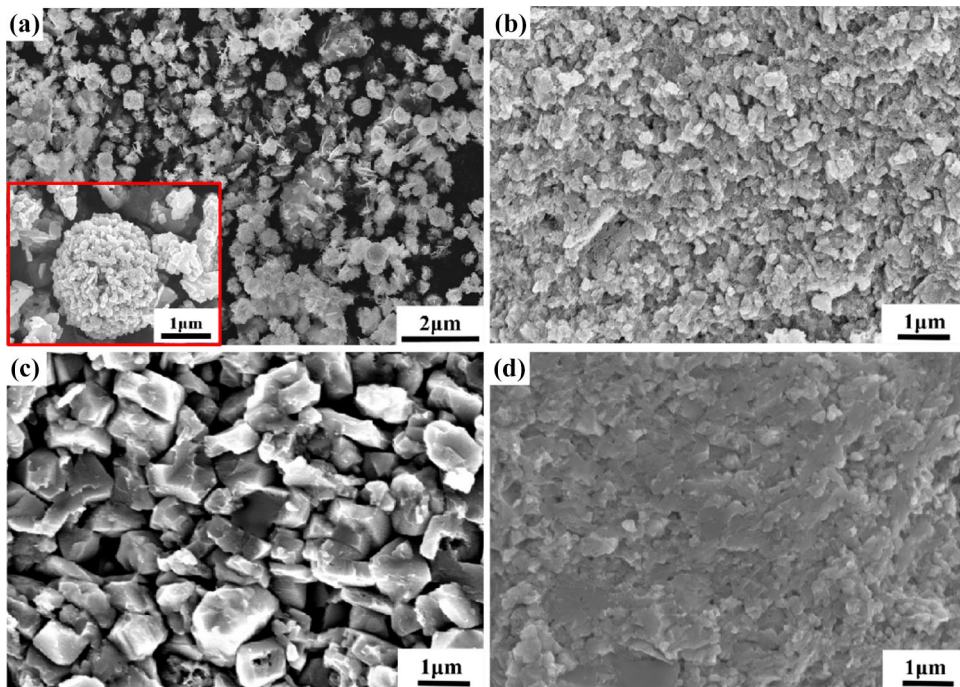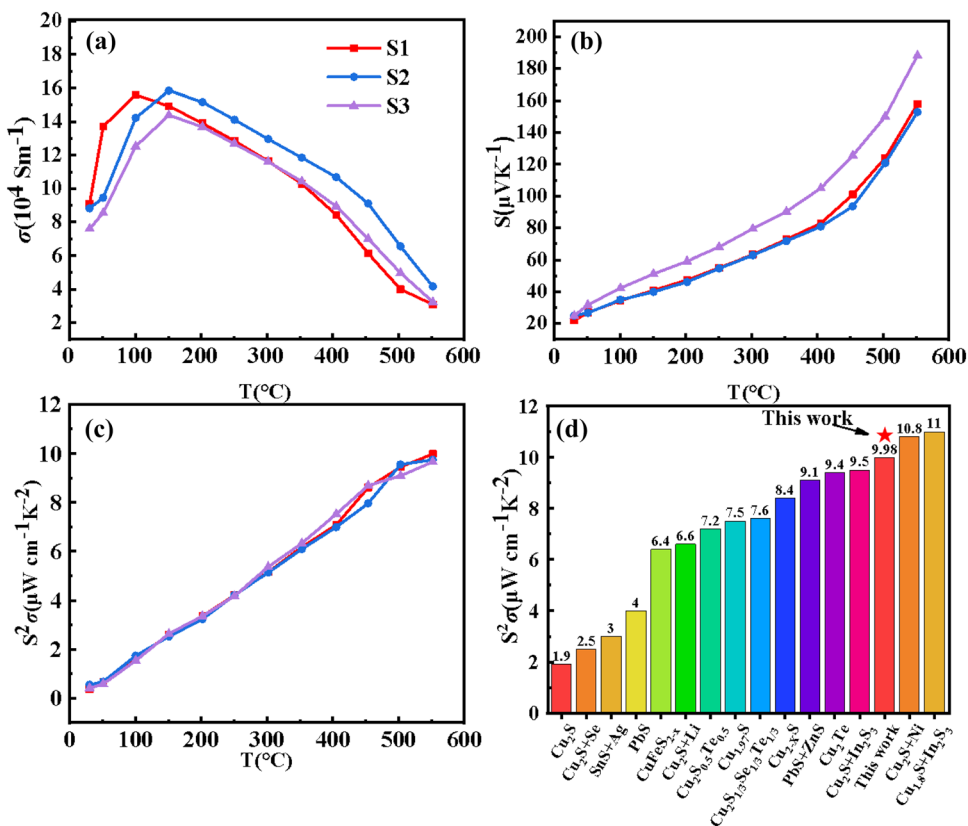

Fig. 3 The temperature-dependent electrical conductivity σ (**a**), Seebeck coefficient S (**b**), and figure of merit ZT (**c**). A comparison of PF of this work with other Cu–S based systems (**d**)

largest ZT over whole testing temperature range and the peak value is 0.78 at 550 °C. Comparing with previous reports on sulfur compounds [55–57], our

samples only exhibit a moderate ZT value, as shown in Fig. 4c. For example, Ge et al. [32] involved the In_2S_3 nanoinclusions into $Cu_{2-x}S$ matrix and
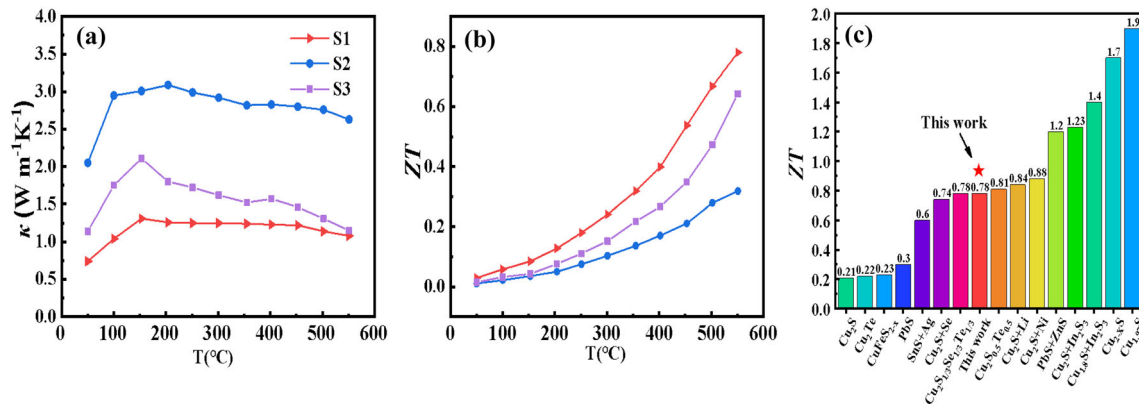
Fig. 4 a The temperature-dependent thermal conductivity κ and **b** figure of merit ZT for the bulk samples. **c** A comparison of ZT of this work with other Cu-S based systems

significantly reduced the thermal conductivity and hence improve the ZT value to 1.4 at 550 °C. For a pure $Cu_{2-x}S$ systems, Zhao et al. [30] prepared the Cu_2S and $Cu_{1.97}S$ polycrystalline bulks by the melt-solidification technique and obtained the extremely low thermal conductivity which is only about one-fourth of our sample S1. However, the bulk samples possess lower *PFs* relative to Ge et al. work and this work and consequently the ZT value is about 1.4 at 550 °C. From the synthesized method, the melt-solidification technique is uneconomical due to its high melting temperatures and long annealing time. This work therefore may provide a probability to facile synthesize the pure $Cu_{2-x}S$ system with high ZT value if the thermal conductivity can be effectively decreased.

Due to the liquid-like properties in copper sulfides, the stability in thermoelectric transport properties has to be considered. Now we made three repeated tests for sample S1. Before each test, the sample is cooled down to room temperature. Surprisingly, comparing to the first test, the electrical conductivity σ drop dramatically and the Seebeck coefficient S is relatively larger at the 2nd and 3rd tests, as clearly shown in Fig. 5a and b. In addition, the σ and S only show a slight difference after the initial test. The *PFs*, however, do not change very much in spite of the large difference in the σ and S, as shown in Fig. 5c. This result may indicate that the electrical performance of copper sulfides is quite stable among the repeated tests.

The drop in electrical conductivity σ after the 1st test might be due to the decrease of charge carrier concentration and the reduction of carrier mobility. As a type of superionic semiconductor [38, 58–60], the copper ions Cu^+ in the samples can migrate easily from the high voltage end to the low voltage end. The electrical conductivity σ, therefore, can be viewed as $\sigma = \sigma_{hole} + \sigma_{ion}$, where σ_{hole} is the majority carrier hole conductivity and σ_{ion} is the ion carrier conductivity, respectively. After the initial test, most of copper ions migrate to one end of the samples, which results in the dramatical reduction on the concentration of copper ions and hence on the σ_{ion}. Additionally, with the temperature increasing, the hole concentration of the samples will also decrease due to sulfur volatilization which causes the reduction of copper vacancies [61–63]. Therefore, it immediately causes the total conductivity σ decreasing in the following electrical test.

These analyses were confirmed by the temperature-dependent carrier concentration and mobility, as shown in Fig. 6. Very clearly, the carrier concentration drops dramatically after the first test. The initial n is about $20 \times 10^{17} cm^3$ at room temperature and reaches over $80 \times 10^{17} cm^3$ at 450 °C, which is almost ten times larger than those in second test (only about $2 \times 10^{17} cm^3$ at room temperature and about $6 \times 10^{17} cm^3$ at 450 °C). These results are in consistent with our previous analyses. However, the carrier mobility only has a slight reduction after the first test. This is quite reasonable result. On the one hand, the carrier concentration decreasing can enhance the hole mobility; on the other hand, the crystal defects increment due to the sulfur volatilization can reduce the hole mobility. Synergistic effect of both factors makes the carrier mobility has no significant change. Consequently, the total electrical conductivity σ, as a product of carrier concentration and mobility, is very larger at

Fig. 5 Repeated tests for the sample S1 in electrical conductivity σ (**a**), Seebeck coefficient S (**b**) and the calculated power factor ZT (**c**)
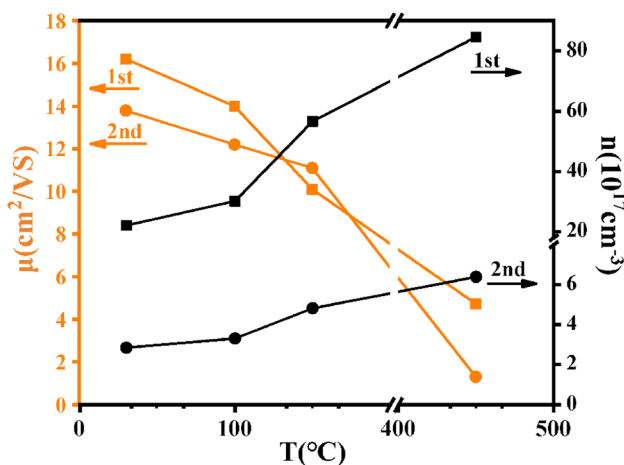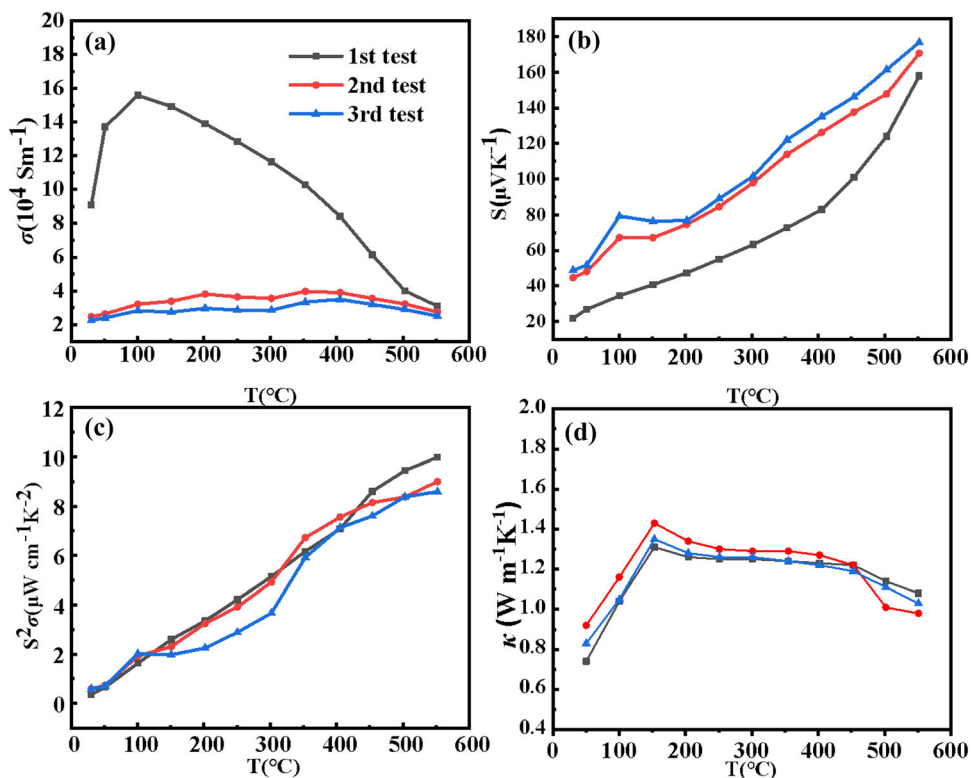

Fig. 6 The carrier concentration n and mobility μ in different temperature

the initial test, while it decreases dramatically at the following tests, as clearly shown in Fig. 5a. Because of the negative correlation with the charge carrier concentration n, the Seebeck coefficient S also is relatively smaller at the first test, as can be seen in Fig. 5b.

For the thermal conductivity κ, we do not observe significant difference among the three tests. An interesting phenomenon is that a peak value of κ occurs around 150 °C, which happens to be the phase

transition temperature of $Cu_{2-x}S$ [31, 37, 38]. The electrical conductivity σ and Seebeck coefficient S also turn downwards after this temperature as shown in Fig. 5a and b. As well known to us, the crystal structure of $Cu_{2-x}S$ ($0 \leq x \leq 0.2$) varies with the atomic ratio of Cu/S. $Cu_{2-x}S$ is monoclinic chalcopyrite (α-Ch) phase at room temperature and transforms to hexagonal chalcopyrite (β-Ch) phase around 150 °C. Our testing result strongly indicates that our sample undergoes a phase transition from α-Ch to β-Ch phase. Figure 6 also shows a sudden change in carrier concentration n and mobility μ around 150 °C [27, 31, 38, 42, 48],. With a more careful observation, we can find another decrease in electrical and thermal conductivity around 450 °C, as shown in Fig. 5a and d. This may be due to the second phase transition from hexagonal phase to cubic phase around 450 °C. These results are well in consistent with the previous works [26, 27, 42, 48].

4 Conclusion

We have synthesized the flower-like spherical $Cu_{2-x}S$ powders by hydrothermal method and densified the bulk samples via HP technique. The results show that

the relative pure copper sulfide can be obtained due to the sulfur volatilization during the sintering process. The bulk samples also exhibit superior thermoelectric performance of $ZT = 0.78$ among the undoped Cu–S based systems. The repeated tests indicate that the samples keep very stable power factor and thermal conductivity, although the carrier concentration n and mobility μ have dramatically change between the different tests. These results suggest that as a kind of liquid-like materials, pure copper sulfide bulk ceramics also can be facilely synthesized and can be very stable on TE performance.

Acknowledgements

Author contributions

XZ contributed to the conception of the study and contributed significantly to analysis and revised the manuscript. FL performed the experiments and the data analyses and wrote the manuscript. JF and HY helped perform the analysis with constructive discussions.

Data availability

The authors confirm that the data supporting the findings of this study are available within the article.

Declarations

Conflict of interest The authors have no conflicts to declare.

References

1. J.F. Li, W.S. Liu, L.D. Zhao, M. Zhou, High-performance nanostructured thermoelectric materials. NPG Asia Mater **2**, 152–158 (2010)
2. L.E. Bell, Cooling, heating, generating power, and recovering waste heat with thermoelectric systems. Science **321**, 1457–1461 (2008)
3. A. Abtahi, S. Johnson, S.M. Park, X.Y. Luo, Z.M. Liang, J.G. Mei, K.R. Graham, Designing pi-conjugated polymer blends with improved thermoelectric power factors. J. Mater. Chem. A **7**, 19774–19785 (2019)
4. Z.H. Wu, S. Zhang, Z.K. Liu, E.Z. Mu, Z.Y. Hu, Thermoelectric converter: strategies from materials to device application. Nano Energy **91**, 106692 (2022)
5. X. Shi, L. Chen, C. Uher, Recent advances in high-performance bulk thermoelectric materials. Int. Mater. Rev. **61**, 379–415 (2016)
6. M. Rakshit, D. Jana, D. Banerjee, General strategies to improve thermoelectric performance with an emphasis on tin and germanium chalcogenides as thermoelectric materials. J. Mater. Chem. A **10**, 6872–6926 (2022)
7. C. Gayner, K.K. Kar, Recent advances in thermoelectric materials. Prog Mater. Sci. **83**, 330–382 (2016)
8. T.J. Zhu, L.P. Hu, X.B. Zhao, J. He, New insights into intrinsic point defects in V_2VI_3 thermoelectric materials. Adv. Sci. **3**, 1600004 (2016)
9. L.P. Hu, T.J. Zhu, X.H. Liu, X.B. Zhao, Point defect engineering of high-performance bismuth-telluride-based thermoelectric materials. Adv. Funct. Mater. **24**, 5211–5218 (2014)
10. G.J. Snyder, E.S. Toberer, Complex thermoelectric materials. Nat. Mater. **7**, 105–114 (2008)
11. W.Y. Chen, X.L. Shi, J. Zou, Z.G. Chen, Thermoelectric coolers: progress, challenges, and opportunities. Small Methods **6**, 2101235 (2022)
12. S.X. Liu, Y. Yu, D. Wu, X. Xu, L. Xie, X.L. Chao, M. Bosman, S.J. Pennycook, Z.P. Yang, J.Q. He, Coherent Sb/CuTe core/shell nanostructure with large strain contrast boosting the thermoelectric performance of n-type PbTe. Adv. Funct. Mater. **31**, 20007340 (2021)
13. X.L. Shi, J. Zou, Z.G. Chen, Advanced thermoelectric design: from materials and structures to devices. Chem. Rev. **120**, 7399–7515 (2020)
14. Z.G. Chen, X. Shi, L.D. Zhao, J. Zou, High-performance SnSe thermoelectric materials: progress and future challenge. Prog Mater. Sci. **97**, 283–346 (2018)
15. M. Madhubant, S. Ashutosh, K.S. Abhishek, Recent advances in designing thermoelectric materials. J. Mater. Chem. C **10**, 12524–12555 (2022)
16. W.K. Li, W.W. Yang, W.W. Sheng, J. Shuai, Research progress of interfacial design between thermoelectric materials and electrode materials. ACS Appl. Mater. Interfaces **15**, 12611–12621 (2023)
17. G.J. Tan, M. Ohta, M.G. Kanatzidis, Thermoelectric power generation: from new materials to devices. Philos. T R Soc. A **377**, 2018450 (2019)

18. Y. Li, G.L. Wang, M. Akbari-Saatlu, M. Procek, H.H. Radamson, Si and SiGe nanowire for micro-thermoelectric generator: a review of the current state of the art. Front. Mater. **8**, 611078 (2021)

19. Y.H. Miao, G.L. Wang, Z.Z. Kong, B.Q. Xu, X.W. Zhao, X. Luo, H.X. Lin, Y. Dong, B. Lu, L.P. Dong, J.R. Zhou, J.B. Liu, H.H. Radamson, Review of Si-Based GeSn CVD growth and optoelectronic applications. Nanomaterials **11**, 2556 (2021)

20. Z.Z. Kong, G.L. Wang, R.R. Liang, J.L. Su, M. Xun, Y.H. Miao, S.H. Gu, J.J. Li, K.H. Cao, H.X. Lin, B. Li, Y.H. Ren, J.F. Li, J. Xu, H.H. Radamson, Growth and strain modulation of GeSn alloys for photonic and electronic applications. Nanomaterials **12**, 981 (2022)

21. M. Noroozi, G. Jayakumar, K. Zahmatkesh, J. Lu, L. Hultman, M. Mensi, S. Marcinkevicius, B. Hamawandi, M.Y. Tafti, A.B. Ergul, Z. Ikonic, M.S. Toprak, H.H. Radamson, Unprecedented thermoelectric power factor in SiGe Nanowires field-effect transistors. Ecs J. Solid State Sc **6**, Q114–Q119 (2017)

22. S. Bathula, M. Jayasimhadri, N. Singh, A.K. Srivastava, J. Pulikkotil, A. Dhar, R.C. Budhani, Enhanced thermoelectric figure-of-merit in spark plasma sintered nanostructured n-type SiGe alloys. Appl. Phys. Lett. **101**, 213902 (2012)

23. L.D. Zhao, H.J. Wu, S.Q. Hao, C.I. Wu, X.Y. Zhou, K. Biswas, J.Q. He, T.P. Hogan, C. Uher, C. Wolverton, V.P. Dravid, M.G. Kanatzidis, All-scale hierarchical thermoelectrics: MgTe in PbTe facilitates valence band convergence and suppresses bipolar thermal transport for high performance. Energy Environ. Sci. **6**, 3346–3355 (2013)

24. T.C. Harman, P.J. Taylor, M.P. Walsh, B.E. LaForge, Quantum dot superlattice thermoelectric materials and devices. Science **297**, 2229–2232 (2002)

25. Z.H. Ge, L.D. Zhao, D. Wu, X. Liu, B.P. Zhang, J.F. Li, J. He, Low-cost, abundant binary sulfides as promising thermoelectric materials. Mater. Today **19**, 227–239 (2016)

26. Q. Xu, B. Huang, Y.F. Zhao, Y.F. Yan, R. Noufi, S.H. Wei, Crystal and electronic structures of Cu_xS solar cell absorbers. Appl. Phys. Lett. **100**, 061906 (2012)

27. Z.H. Ge, B.P. Zhang, Y.X. Chen, Z.X. Yu, Y. Liu, J.F. Li, Synthesis and transport property of $Cu_{1.8}S$ as a promising thermoelectric compound. Chem. Commun. **47**, 12697–12699 (2011)

28. W.D. Liu, L. Yang, Z.G. Chen, J. Zou, Promising and eco-friendly Cu_2X-Based thermoelectric materials: Progress and Applications. Adv. Mater. **32**, 1905703 (2020)

29. G. Dennler, R. Chmielowski, S. Jacob, F. Capet, P. Roussel, S. Zastrow, K. Nielsch, I. Opahle, G.K.H. Madsen, Are binary copper Sulfides/Selenides really New and Promising Thermoelectric Materials? Adv. Energy Mater. **4**, 1301581 (2014)

30. L. Zhao, X. Wang, F.Y. Fei, J. Wang, Z. Cheng, S. Dou, J. Wang, G.J. Snyder, High thermoelectric and mechanical performance in highly dense $Cu_{2-x}S$ bulks prepared by a melt-solidification technique. J. Mater. Chem. A **3**, 9432–9437 (2015)

31. Y. He, T. Day, T. Zhang, H. Liu, X. Shi, L. Chen, G.J. Snyder, High thermoelectric performance in non-toxic earth-abundant copper sulfide. Adv. Mater. **26**, 3974–39780 (2014)

32. Z.H. Ge, X. Chong, D. Feng, Y.X. Zhang, Y. Qiu, L. Xie, P.W. Guan, J. Feng, J. He, Achieving an excellent thermoelectric performance in nanostructured copper sulfide bulk via a fast doping strategy. Mater. Today Phys. **8**, 71–77 (2019)

33. Q.L. Meng, S. Kong, Z. Huang, Y. Zhu, H.C. Liu, X. Lu, P. Jiang, X. Bao, Simultaneous enhancement in the power factor and thermoelectric performance of copper sulfide by In_2S_3 doping. J. Mater. Chem. A **4**, 12624–12629 (2016)

34. Y.X. Zhang, J. Feng, Z.H. Ge, Enhanced thermoelectric performance of $Cu_{1.8}S$ via lattice softening. Chem. Eng. J. **428**, 131153 (2022)

35. Z.H. Zheng, X.L. Shi, D.W. Ao, W.D. Liu, Y.X. Chen, F. Li, S. Chen, X.Q. Tian, X.R. Li, J.Y. Duan, H.L. Ma, X.H. Zhang, G.X. Liang, P. Fan, Z.G. Chen, Rational band engineering and structural manipulations inducing high thermoelectric performance in n-type $CoSb_3$ thin films. Nano Energy **81**, 105683 (2021)

36. Y. Yao, B.P. Zhang, J. Pei, Y.C. Liu, J.F. Li, Thermoelectric performance enhancement of Cu_2S by Se doping leading to a simultaneous power factor increase and thermal conductivity reduction. J. Mater. Chem. C **5**, 7845–7852 (2017)

37. Y. He, P. Lu, X. Shi, F. Xu, T. Zhang, G.J. Snyder, C. Uher, L. Chen, Ultrahigh Thermoelectric performance in Mosaic crystals. Adv. Mater. **27**, 3639–3644 (2015)

38. P. Lukashev, W.R.L. Lambrecht, T. Kotani, M. Van Schilfgaarde, Electronic and crystal structure of $Cu_{2-x}S$: full-potential electronic structure calculations. Phys. Rev. B **76**, 195202 (2007)

39. L.J. Wu, Q.P. Meng, C. Jooss, J.C. Zheng, H. Inada, D. Su, Q. Li, Y.M. Zhu, Origin of Phonon Glass-Electron Crystal Behavior in Thermoelectric Layered Cobaltate. Adv. Funct. Mater. **23**, 5728–5736 (2013)

40. H.L. Liu, X. Shi, F.F. Xu, L.L. Zhang, W.Q. Zhang, L.D. Chen, Q. Li, C. Uher, T. Day, G.J. Snyder, Copper ion liquid-like thermoelectrics. Nat. Mater. **11**, 422–425 (2012)

41. C.L. Wan, Y.F. Wang, N. Wang, W. Norimatsu, M. Kusunoki, K. Koumoto, Development of novel thermoelectric materials by reduction of lattice thermal conductivity. Sci. Technol. Adv. Mater. **11**, 044306 (2010)

42. Y.X. Sun, L.L. Xi, J. Yang, L.H. Wu, X. Shi, L.D. Chen, J. Snyder, J.H. Yang, W.Q. Zhang, The "electron crystal"

behavior in copper chalcogenides Cu_2X (X = Se, S). J. Mater. Chem. A **5**, 5098–5105 (2017)

43. D. Zhang, J.Y. Yang, Q.H. Jiang, L.W. Fu, Y. Xiao, Y.B. Luo, Z.W. Zhou, Ternary $CuSbSe_2$ chalcostibite: facile synthesis, electronic-structure and thermoelectric performance enhancement. J. Mater. Chem. A **4**, 4188–4193 (2016)

44. T. Ohtani, M. Motoki, K. Koh, K. Ohshima, Synthesis of binary copper chalcogenides by mechanical alloying. Mater. Res. Bull. **30**, 1495–1504 (1995)

45. N. Nandihalli, D.H. Gregory, T. Mori, Energy-Saving pathways for Thermoelectric Nanomaterial Synthesis: Hydrothermal/Solvothermal, Microwave-Assisted, Solution-Based, and Powder Processing. Adv. Sci. **9**, 2106052 (2022)

46. Y.X. Zhao, H.C. Pan, Y.B. Lou, X.F. Qiu, J.J. Zhu, C. Burda, Plasmonic Cu2-xS nanocrystals: Optical and Structural Properties of copper-deficient copper(I) Sulfides. J. Am. Chem. Soc. **131**, 4253–4261 (2009)

47. Z.P. Liu, D. Xu, J.B. Liang, J.M. Shen, S.Y. Zhang, Y.T. Qian, Growth of Cu_2S ultrathin nanowires in a binary surfactant solvent. J. Phys. Chem. B **109**, 10699–10704 (2005)

48. P. Roy, S.K. Srivastava, Nanostructured copper sulfides: synthesis, properties and applications. Crystengcomm **17**, 7801–7815 (2015)

49. L.D. Zhao, V.P. Dravid, M.G. Kanatzidis, The panoscopic approach to high performance thermoelectrics. Energy Environ. Sci. **7**, 251–268 (2014)

50. K.F. Li, Q.J. Wang, X.Y. Cheng, T. Lv, T.K. Ying, Hydrothermal synthesis of transition-metal sulfide dendrites or microspheres with functional imidazolium salt. J. Alloy Compd. **504**, L31–L35 (2010)

51. G. Li, M.Y. Liu, H.J. Liu, Controlled synthesis of porous flowerlike Cu_2S microspheres with nanosheet-assembly. CrystEngComm **13**, 5337–5341 (2011)

52. L.D. Zhao, J. He, S. Hao, C.I. Wu, T.P. Hogan, C. Wolverton, V.P. Dravid, M.G. Kanatzidis, Raising the Thermoelectric performance of p-Type PbS with Endotaxial Nanostructuring and Valence-Band Offset Engineering using CdS and ZnS. J. Am. Chem. Soc. **134**, 16327–16336 (2012)

53. F.H. Shen, Y.Y. Zheng, L. Miao, C.Y. Liu, J. Gao, X.Y. Wang, P.F. Liu, K. Yoshida, H.F. Cai, Boosting high thermoelectric performance of Ni-Doped $Cu_{1.9}S$ by significantly reducing Thermal Conductivity. Acs App Mater Inter **12**, 8385–8391 (2020)

54. K.P. Zhao, C.X. Zhu, P.F. Qiu, A.B. Blichfeld, E. Eikeland, D.D. Ren, B.B. Iversen, F.F. Xu, X. Shi, L.D. Chen, High thermoelectric performance and low thermal conductivity in $Cu_{2-y}S_{1/3}Se_{1/3}Te_{1/3}$ liquid-like materials with nanoscale mosaic structures. Nano Energy **42**, 43–50 (2017)

55. P.P. Li, Z.Y. Jin, Y.M. Qian, Z.W. Fang, D. Xiao, G.H. Yu, Supramolecular confinement of single Cu atoms in hydrogel frameworks for oxygen reduction electrocatalysis with high atom utilization. Mater. Today **35**, 78–86 (2020)

56. J.H. Li, Q. Tan, J.F. Li, Synthesis and property evaluation of $CuFeS_{2-x}$ as earth-abundant and environmentally-friendly thermoelectric materials. J. Alloy Compd. **551**, 143–149 (2013)

57. M.J. Guan, P.F. Qiu, Q.F. Song, J. Yang, D.D. Ren, X. Shi, L.D. Chen, Improved electrical transport properties and optimized thermoelectric figure of merit in lithium-doped copper sulfides. Rare Met. **37**, 282–289 (2018)

58. C. Naşcu, I. Pop, V. Ionescu, E. Indrea, I. Bratu, Spray pyrolysis deposition of CuS thin films. Mater. Lett. **32**, 73–77 (1997)

59. M.T.S. Nair, L. Guerrero, P.K. Nair, Conversion of chemically deposited CuS thin films to and by annealing. Semicond. Sci. Tech. **13**, 1164–1169 (1998)

60. K.P. Zhao, P.F. Qiu, X. Shi, L.D. Chen, Recent advances in Liquid-Like Thermoelectric materials. Adv. Funct. Mater. **30**, 1903867 (2020)

61. X.Y. Zhou, Y.C. Yan, X. Lu, H.T. Zhu, X.D. Han, G. Chen, Z.F. Ren, Routes for high-performance thermoelectric materials. Mater. Today **21**, 974–988 (2018)

62. X.L. Shi, A.Y. Wu, T.L. Feng, K. Zheng, W.D. Liu, Q. Sun, M. Hong, S.T. Pantelides, Z.G. Chen, J. Zou, High thermoelectric performance in p-type Polycrystalline Cd-doped SnSe achieved by a combination of Cation Vacancies and localized Lattice Engineering. Adv. Energy Mater. **9**, 1803242 (2019)

63. W.D. Liu, X.L. Shi, R. Moshwan, L. Yan, Z.G. Chen, J. Zou, Solvothermal synthesis of high-purity porous $Cu_{1.7}Se$ approaching low lattice thermal conductivity. Chem. Eng. J. **375**, 121996 (2019)